行政院國家科學委員會專題研究計畫　成果報告

廢矽藻土資源再生為多孔性材料及其應用於環境荷爾蒙之處理(II)

計畫類別：個別型計畫
計畫編號：NSC93-2211-E-041-008-
執行期間：93 年 08 月 01 日至 94 年 07 月 31 日
執行單位：嘉南藥理科技大學環境工程與科學系(所)

計畫主持人：蔡文田

報告類型：精簡報告

處理方式：本計畫可公開查詢

中　華　民　國 94 年 10 月 27 日

行政院國家科學委員會補助專題研究計畫 ■ 成 果 報 告 □期中進度報告

廢矽藻土資源再生為多孔性材料及其應用於環境荷爾蒙之處理**(II)**

計畫類別：■ 個別型計畫　　□ 整合型計畫
計畫編號：NSC **93－2211－E－041－008**
執行期間：**93 年 08 月 01 日至 93 年 07 月 31 日**

計畫主持人：**蔡文田**
共同主持人：
計畫參與人員：**賴智濰、蘇庭毅、張正弘、謝國鎔**

成果報告類型(依經費核定清單規定繳交)：■精簡報告　□完整報告

本成果報告包括以下應繳交之附件：(無)
□赴國外出差或研習心得報告一份
□赴大陸地區出差或研習心得報告一份
□出席國際學術會議心得報告及發表之論文各一份
□國際合作研究計畫國外研究報告書一份

處理方式：除產學合作研究計畫、提升產業技術及人才培育研究計畫、列管計畫及下列情形者外，得立即公開查詢
□涉及專利或其他智慧財產權，□一年□二年後可公開查詢

執行單位：**嘉南藥理科技大學環境工程與科學系**

中　華　民　國　94 年　10 月　27 日

行政院國家科學委員會專題研究計畫成果報告

廢矽藻土資源再生為多孔性材料及其應用於環境荷爾蒙之處理(II)

計畫編號：NSC 93-2211-E-041-008
執行期限：93 年 8 月 1 日至 94 年 7 月 31 日
主持人：蔡文田 嘉南藥理科技大學環境工程與科學系
計畫參與人員：賴智濰、蘇庭毅、張正弘
嘉南藥理科技大學環境工程與科學系

一、中文摘要

本研究之目的乃利用氫氟酸做為含浸的活化劑，配合不同活化參數(濃度、時間、溫度)進行純矽藻土及廢矽藻土之化學活化。研究結果顯示純矽藻土化學活化之最佳條件為活化濃度 2.5N、活化時間 0.5 hr、活化溫度 60℃、樣品重/活化液比為 5/100 的條件下，S_{BET} 可由 3.81 m^2/g 上升至 7.04 m^2/g 提升近 2 倍，孔洞體積也由 0.0161cm^3/g 提升至 0.0560cm^3/g。廢矽藻土化學活化之最佳條件為活化濃度 2.5N、活化時間 0.5 hr、活化溫度 25℃、樣品重/活化液比為 5/100 的條件下，S_{BET} 可由 0.43m^2/g 上升至 4.85m^2/g 提升了十倍，孔洞體積也由 0.0036cm^3/g 提升至 0.0430cm^3/g。對活化後之產物做其物理/化學特性分析，包括表面積/孔洞體積、掃描式電子顯微鏡(SEM)、X 光繞射(XRD)、傅利葉紅外線光譜(FTIR)及主要元素，顯示所得之產物從 N_2 之等溫吸脫附分析大致為中-巨孔性結構(Type II 及 IV)。進一步以活化後最佳物性產物對環境賀爾蒙丙二酚 A 進行吸附實驗，並利用 Langmuir 及 Freundlich 等溫吸附模式進行迴歸，結果顯示此礦物性吸附劑對此屬疏水性環境有機化合物並沒有很高的吸附容量，主要係因靜電排斥作用力所致。

關鍵字：矽藻土；化學活化；氫氟酸；特性

Abstract

The objective of this study was to use hydrofluoric acid (HF) as etching agent for chemically activating fresh and spent diatomaceous earths under different activation parameters including impregnation concentration, holding time, temperature etc. The experimental results showed that the optimal activation conditions for fresh diatomaceous earth seemed to be at the concentration of HF 2.5 N, holding time of 0.5 hr, temperature of 60 ℃ and sample/solution weight ratio of 5/100. Under these conditions, the main physical properties of resulting product were BET surface area of 7.04 m^2/g and total pore volume of 0.0560 cm^3/g as compared to 3.81 m^2/g and 0.0161 cm^3/g of its precursor, respectively. Compared to the foregoing, the optimal activation conditions for spent diatomaceous earth seemed to be similar to those of fresh diatomaceous earth except temperature at 25 ℃. Under these conditions, the main physical properties of resulting product were BET surface area of 4.85 m^2/g and total pore volume of 0.0430 cm^3/g as compared to 0.43 m^2/g and 0.0036 cm^3/g of its precursor, respectively.

The physical and chemical properties characterizations of some resulting products obtained in the chemical activation were further examined using the analyses of surface area/pore volume, scanning electron microscopy (SEM), X-ray diffraction (XRD), Fourier infrared spectroscopy (FTIR) and main elements. The analytical results showed that these samples are basically characteristic of types II and IV base on the N_2 isotherm, indicating mesoporous-macroporous structure. Finally, the optimal porous product was used as a mineral adsorbent for environmental hormone bisphenol-A, showing that it has a poor adsorption capacity for the removal of this hydrophobic organic compound from the aqueous solution based on the fittings of Langmuir and Freundlich isotherms, mainly due to the electrostatic repulsion interaction between the adsorbent with negatively-charged surface and adsorbate with neutrally-polar structure.

Keywords: Diatomaceous earth ; chemical activation；hydrofluoric acid；characterization

(本研究計畫成果據以投稿 SCI 論文三篇，其中二篇已接受，作為本計畫成果報告，另一篇投稿於 Bioresource Technology, 標題為” Chemical treatment of spent diatomaceous earth from beer brewing”，正審查中，未列於此報告中)。

Ms. No.:JCIS-05-1300 (Journal of Colloid and Interface Science, Accepted)

Characterization and Adsorption Properties of Diatomaceous Earth Modified by Hydrofluoric Acid Etching

Wen-Tien Tsai *, Chi-Wei Lai, Kuo-Jong Hsien

Department of Environmental Engineering and Science, Chia Nan University of Pharmacy and Science, Tainan 717, Taiwan

Abstract

This work was to study the chemical modification of diatomaceous earth (DE) by using hydrofluoric acid (HF) solution. Under the experimental conditions investigated, it was found that the method by HF under controlled conditions significantly etched to proceed inwardly into the interior of the existing pore structure in the clay mineral due to its high content of silica, leaving a framework possessing a larger BET surface area (*ca.* 10 m^2 g^{-1}) in comparison with that (*ca.* 4 m^2 g^{-1}) of its precursor (i.e., DE). Further, the results indicated that the HF concentration has a more determining factor in creating more open pores than other process parameters (i.e., temperature, holding time and solid/liquid ratio) do. This observation was also in close agreement with the examinations on the silicon analysis, scanning electron microscopy (SEM), X-ray diffraction (XRD) and Fourier transform infrared spectroscopy (FTIR). In the adsorption tests, the adsorption kinetics and isotherm of methylene blue onto the resulting clay adsorbent can be well described with the pseudo-second order reaction model and the Freundlich model, respectively.

Keywords: Diatomaceous earth; Chemical modification; Hydrofluoric acid; Characterization; Adsorption

* To whom correspondence should be addressed. Tel.: +886-6-2660393. Fax: +886-6-2669090. E-mail address: wwtsai@mail.chna.edu.tw

1. Introduction

Diatomaceous earth (DE), or diatomite typically consists of 87-91% silicon dioxide (SiO_2), with significant quantities of alumina (Al_2O_3) and ferric oxide (Fe_2O_3) [1]. Due to its specific properties (i.e., porous structure, high silica content, low density, low conductivity coefficient, *etc*.) [1-2], DE has extensively been applied for many fields such as filter aid [3], adsorbent [4-10], insulating material [11], catalyst support or carrier [12], and natural insecticide or grain protectant [13] etc. It is noted that diatomite has only weak adsorption capacity but possesses excellent absorption power because of its macroporous structure. Thus one of main end uses of diatomite is as absorbent for fluids such as acid, liquid fertilizer, oil, water, and alcohol [1].

Commercial diatomite is generally produced from natural diatomite by the calcination processing at about 900 ℃ [1]. However, in many cases the clay mineral can be chemically treated or activated to modify their pore structure and/or the surface chemistry of the solid. Acid activation of clay mineral (e.g., montmorillomite, bentonite) is a commonly chemical modification to enhance its adsorption capacity and to give it certain properties for desirable applications [14-22]. It is well known that silica (SiO_2), which is the most abundant component in the diatmoaceous earth, is quite inert, being attacked only by strong alkali (e.g., NaOH) or hydrofluoric acid (HF) as a consequence of the formation of soluble product (i.e., SiO_3^{2-} or SiF_6^{2-}) [23]. Therefore, the wet cleaning and etching processes of wafers in the semiconductor manufacturing industry are commonly carried out by the use of NaOH or HF [24, 25].

Recently, we have described the NaOH activation of spent diatomaceous earth, with a complete characterization and adsorption properties of the resulting solids [22, 26]. The pore textures of some resulting solids thus obtained are mesoporous, indicating that they belong to type IV according to the Brunauer, Deming, Deming and Teller (BDDT) classification [27]. With respect to the activation of clay mineral using HF, the information published is very scarce. This study was further stimulated by the etching reaction between

SiO_2 and HF. The main objectives of this work were to study the feasibility of utilizing diatomaceous earth as a precursor in the production of silica-like adsorbent by the physical and chemical characterization, and further evaluate its adsorption properties for the removal of methylene blue from aqueous solution at 25 ℃.

2. Materials and Methods

2.1. Materials

The diatomaceous earth was obtained from Shan-Hua Factory of Taiwan Tobacco & Liquor Co. (Tainan, Taiwan). The precursor was a calcined product (Grade No.: 577; Celite Co., USA) with a median particle size of 20.8 μm. The typical chemical compositions from the manufacturer's brochure mainly consist of 92.0% of SiO_2, 3.3% of Al_2O_3 and 1.3 % of Fe_2O_3. The sample was first dried in the oven (105 ℃) at least 2 h, and then cooled to room temperature for further characterization and chemical activation. Hydrofluoric acid (HF, 48%), which was purchased from Merck Co. (Germany) with grade for analysis, was selected as chemical activator in this study to etch the dried sample for the purpose of creating more finely pores. The adsorbate used in the adsorption experiments was methylene blue (i.e., basic blue 9; C.I. 52015) with purity of min. 99 % from Sigma Chemical Co. (U.S.A.).

2.2. Chemical modification

The apparatus and chemical modification method with HF employed in the present work are similar to those for chemical activation with NaOH as reported previously [22, 26]. It is noted that HF is actually a very weak acid, and the fluoride ion is highly electronegative. The etching reaction between the glass bottle (mainly composed of SiO_2) and HF will thus occur. Therefore, the solution containing diatomite and HF was first prepared in the polypropylene (PP) plastic bottle because of its good resistance to the etching dissolution up to 50% of HF at ambient temperature [28], and then bathed in silicone oil, which was held in the Pyrex glass for the purpose of heating on the hot plate. Under various concentrations

(0.2-2.5 N of HF), adsorbent dosages (2.5-12.5 grams of 100 ml HF solution), holding times (0.5 ~ 8.0 h) and temperatures (25 ~ 100 ℃), the chemical modification of the dried diatomite by HF was carried out on a laboratory stirrer/hot plate (Model No.: PC-420; Corning Co., USA) with boiler-reflux condenser. Afterward, the sample solution was filtered in a vacuum filter flask and washed sequentially with deionized water five times to remove the ions and other residues. The resulting solid was finally dried at 105 ℃ for 24 h, and stored in the desiccator after drying.

2.3. Physical Characterizations

The pore structures of diatomaceous earth and its HF-modified products (denoted as MDE) relating to surface areas, total pore volume and pore size distribution were obtained by measuring their nitrogen adsorption-desorption isotherms at –196 ℃ in a surface area & porosity analyzer (Model ASAP 2010; Micromeritics Co., U.S.A.). In order to evaluate its precision, the pore structure of diatomaceous earth used as a reference sample was repeatedly measured at least two times before being measured in the experiments. As shown in Table 1, this automatic instrument has a high precision based on the standard deviations. From the data of total pore volume (V_t) and true density (ρ_s), the particle density (ρ_p) and porosity (ε_p) can be further obtained [29, 30]. A Siemens D5000 powder diffractometer (Cu-Kα radiation) was used to obtain powder XRD patterns for the purpose of observing the changes in crystallinity between the samples. The surface textures of the samples were made using the scanning electron microscopy (SEM) by a JEOL JXA-840 (JEOL Co., Japan) apparatus.

2.4. Chemical Characterizations

The carbon/hydrogen/nitrogen (C/H/N) contents of diatomaceous earth and its HF-modified products (denoted as MDE) were used as a means of examining the residues of the resulting products in the chemical modification processes. The C/H/N elemental analysis of the samples (1-3 mg) was performed by using an elemental analyzer (model CHN-O-RAPID, Heraeus Co., Germany). For each analysis, the standard sample (i.e.,

acetanilide) was first analyzed for checking the experimental error within ±1 %. In order to measure the quantity of silicon leached out from the modified diatomaceous earths, the silicon contents of diatomaceous earth and its HF-modified products (denoted as MDE) were analyzed using an inductively coupled plasma-atomic emission spectrometer (model ICAP 9000, Jarrell-Ash Co., U.S.A.). Prior to analysis, the samples were first digested in the concentrated nitric acid/hydrofluoric acid solution to form the solution samples. The Fourier transform infrared spectroscopy (FTIR) analysis has been used for the observation of functional groups on the surface of the samples (KBr). The spectrum was measured and recorded (500 ~ 2000 cm^{-1}) on a spectrometer (model DA 8.3, Bomen Co., Canada).

2.5. Adsorption tests

Adsorption behaviors of the optimal modified solid (i.e., MDE-2.5N) were tentatively determined to evaluate their potentials for removal of methylene blue from aqueous solution at 25.0 ℃. Adsorption experiments were carried out in a *ca.* 3 dm^3 stirred batch adsorber with four baffles as similarly described in our previous studies [22, 26]. In the present study, the adsorption solution was maintained at the same conditions (e.g. solution volume = 2 dm^3, MDE adsorbent dosage= 0.5 g /2.0 dm^3, agitating speed = 400 rpm, and pH = 7.0) with an outer circulating-water bath for the adsorbability of the basic dye under various initial concentrations (4-12 mg dm^{-3}). For a preliminary comparison, the adsorption behavior of diatomaceous earth under initial methylene blue concentration of 10 mg dm^{-3} was also carried out at the same solution conditions. The concentration of the dye filtrate was determined immediately through the use of a spectrophotometer (Hitachi UV-2001) at the wavelength of UV-maximum (λ_{max}) of 661 nm. The amounts of methylene blue adsorbed onto the two adsorbents were determined as follows:

$$q_t = (C_o - C_t) \cdot V/W \qquad (1)$$

where C_o and C_t are the initial and liquid-phase concentrations (mg dm^{-3})of dye solution at *t* (min), respectively, V is the volume of dye solution (*ca.* 2 dm^3), and W is the mass of dry

adsorbent used (g).

3. Results and Discussion

3.1. Physical Characterization

Generally, the Brunauer, Emmett and Teller (BET) equation has been used for measuring and comparing the specific surface areas of a variety of adsorbents from their nitrogen adsorption-desorption isotherms at 77 K (–196 ℃) [27]. In the present study, the BET surface area was regarded as a comparative factor of determining the degree of pore properties of the modified diatomaceous earths.

According to the previous study [22], it was found that the NaOH concentration seems to have the most efficient effect on the development of pores in the base-activated samples. Shown in Fig. 1 is the effect of HF concentration on the BET surface areas of the resulting solids prepared under the fixed holding time of 0.5 h and solid/liquid ratio of 5 g/100 ml. In the HF-modifed diatomaceous earth series, the pore property at 60 ℃ is slightly larger than that at 80 ℃. Also, the increase in pore property seems to be proportional to the HF concentration. The observation is consistent with H_2SO_4-activated solids [22] and HaOH-activated solids [22, 26]. The optimal BET surface area (*ca.* 10 m^2 g^{-1}) can be obtained at the temperature of 60 ℃, HF concentration of 2.5 N, holding time of 0.5 h and solid/liquid ratio of 5 g/100 ml. As compared to the data in Table 1, it can be seen that the HF has an etching performance to create more open pores, thus resulting in larger surface areas. The results were further confirmed from the nitrogen adsorption-desorption isotherms and pore size distributions shown in Figs. 2 and 3, respectively. On the basis of the BDDT classification, the patterns of adsorption-desorption isotherms in Fig. 2 belong to a typical type II, indicating that the diatomaceous earth and their modified solids should be still macroporous powders or powers with pore diameters larger than micropores [31]. The foregoing results may be further observed in the pore size distribution curves based on pore areas of the Barrett-Joyner-Halenda (BJH) desorption branch in the measurement of N_2

isotherms, as shown in Fig. 3. It is seen that the pores of these clay samples (incl., DE, MDE-1.0 N, and MDE-2.5 N) have a heterogeneous distribution of pore diameters with major pore ranges below about 100 Å, which may be useful for their possible applications in adsorption of component with large molecular size from liquid phase.

The effects of temperature, holding time and solid/liquid ratio under specified modification conditions on the BET surface areas of the resulting products are shown in Figs. 4-6, respectively. It seems that these modification parameters play a less important role in the production of the porous materials prepared from the diatomaceous earth by HF. For example, with increase in the temperature from 25 ℃ to 100 ℃ (boiling) at a HF concentration of 1.0 N, the resulting solids have almost the same BET surface area (seen in Fig. 4). Also shown in Fig. 6, the BET surface areas of the resulting solids tend towards gradual decrease with increasing adsorbent dosage. The decrease in pore property is probably due to less etching rate of reaction at a higher solid/liquid ratio.

SEM micrographs of the diatomaceous earth (DE) and optimal sample (i.e., MDE-2.5 N) are illustrated in Fig. 7, showing a great difference between the surface textures of these samples. The porous structure examination of the precursor DE can be clearly seen in the SEM photograph (left, Fig. 7), revealing the variety of rigid shapes and macropores/open voids that give the diatomaceous earths with high ability to trap solids or residues for separation from clear liquids. Obviously, the pores can be developed and further enhanced by the chemical modification during the etching reaction by HF, which results in flaws, cracks, crevices, and small pores in the small particles shown in Fig. 7 (right).

In order to observe changes in crystallinity as a result of the HF-modification, the powder XRD patterns of some typical samples (incl. DE, MDE-0.2 N, MDE-0.5 N, MDE-1.0 N, MDE-1.5 N, and MDE-2.5 N) are shown in Fig. 8. It is clear that the XRD patterns having the maximum silica peak at about 22.0 degree of 2θ are not significantly modified by HF etching, showing that the precursor has a high resistance to HF attack, and that its pore property is thus not enhanced under chemical modification conditions. This phenomenon

also seems to be in line with the data shown in Fig. 1, in which the increase in BET surface area is only from 3.9 to 9.4 $m^2 g^{-1}$ with increasing HF concentration from 0.2 to 2.5 N.

3.2. Chemical Characterization

Table 2 presents the contents of carbon (C), hydrogen (H), nitrogen (N), and silicon (Si) of MDE series. Compared with those of DE (Table 2), the MDE displayed a very distinctive chemical composition. Their carbon contents were significantly lower probably due to the partial dissolution of carbonates. It is particularly interesting that the MDE series possessed a fairly lower silicon contents than that of DE, showing that the etching reaction between silica and HF could occur, and that is also gave rise to their larger pore properties as shown in Figs. 1-2. Notably, the etching degree, indicative of silicon content, tends to increase with increasing in HF concentration

The study of the HF modified solids by FTIR spectroscopy confirms the presence of silica in them. The spectra of the samples DE and MDE series treated with 0.2, 0.5, 1.0, 1.5, and 2.5 N are displayed in Figure 9. Clearly, there are no significant differences between characteristic bands ranging from 1400 and 400 cm^{-1} (i.e., 1200-1000, and 795 cm^{-1}) due to silicates structure [16, 33], which was also seen in the XRD peaks at 2θ of 21-22 degree (Fig. 8). This is consistent with the data on the BET surface areas shown in Fig. 1. The wide bands centered at *ca.* 1090 cm^{-1} should be due to Si-O-Si in-plane vibration (asymmetric stretching). Similar observations can be seen at *ca.* 795 cm^{-1}, which are also characteristic of silica. Again, the weak absorption peak at 616 cm^{-1} was possibly attributed to Si-O deformation and Al-O stretching [32].

3.3. Adsorption property

In the adsorption experiments, the optimal solid MDE-2.5 N was chosen as a representative adsorbent. The effect of initial dye concentration on the adsorption intake of methylene blue at the adsorbent dosage of 0.5 g 2.0 dm^{-3}, initial pH of 7.0, temperature of 25 ℃ and mixing speed of 400 rpm was carried out, and further analyzed using

pseudo-second-order kinetic model with its linear form as studied previously [22, 26]:

$$t / q_t = 1/(k . q_e^2) + (1/q_e) . t \quad (2)$$

where k is the pseudo-second order rate constant (g $mg^{-1}min^{-1}$), q_e is the amount of methylene blue adsorbed at equilibrium (mg g^{-1}), q_t is the amount of methylene blue adsorbed at time t (mg g^{-1}). Rate parameters, k and q_e, can be directly obtained from the intercept and slope of the plot of (t/q_t) against t. Values of k and q, computed from Eq. (2), are listed in Table 3. As a preliminary evaluation, the starting precursor DE was used as another adsorbent for the adsorption of methylene blue with the initial concentration 10.1 mg/L. From the data in Table 3, it is clear that the kinetics of methylene blue adsorption on the HF-modified adsorbent follows this model with the regression coefficients of higher than 0.99 in this study. Also, it is consistent with the results based on the data in Fig. 2, namely, the adsorbent MDE-2.5N has a higher capacity for the adsorption of methylene blue than that of the adsorbent DE because of the larger BET surface area in the former.

Based on the trend on the adsorption capacity (i.e., q_e) vs. equilibrium concentration (i.e., C_e) in Table 3, the Freundlich model was used to describe the adsorption isotherm because of its superiority to the Langmuir model from the fitting results:

$$q_e = K_F \cdot C_e^{1/n} \quad (3)$$

Table 4 presents the results of Freundlich isotherm values by using the adsorption capacity data (Table 3) at 25 ℃. Obviously, it can be seen that the uptake amount of the modified clay adsorbent is significantly lower than those of the NaOH-activated adsorbents as reported previously at the same C_e [22, 26]. As also illustrated in Table 4, the value of 1/n is close to 1.0 that indicated a linear adsorption isotherm.

4. Conclusions

In conclusion, the etching treatment of diatomaceous earth changes the surface properties by using HF solution. It was found that the HF concentration is a determining factor in

creating more open pores, thus resulting in larger surface area as compared to other parameters like temperature, holding time and solid/liquid ratio. The BET surface area of the optimal resulting solids thus obtained in the study is about 10.0 m^2 g^{-1}, which is significantly larger than that (i.e., 3.8 m^2 g^{-1}) of the starting material. This observation was also in close agreement with the results on the elemental analysis, SEM, XRD and FTIR. In contrast, the optimal product thus prepared was used as mineral adsorbent for adsorption of methylene blue (basic dye 9) at 25 ℃. The adsorption kinetics and isotherm of methylene blue under various initial dye concentrations can be well described with the pseudo-second order reaction model and the Freundlich model, respectively.

Acknowledgement

This research was supported by NSC (National Science Council), Taiwan, under contract number NSC 93-2211-E-041-008.

References

[1] K.R. Engh, in: M. Howe-Grant (Ed.), Kirk-Othmer Encyclopedia of Chemical Technology, 4th ed., John Wiley & Sons, New York, 1993, Vol. 8, p. 108.

[2] J.F. Lemonas, Am. Ceramic Soc. Bull. 76 (1997) 92.

[3] E.I. El-Shafey, M. Gameiro, P. Correia, J. de Carvalho, Sep. Sci. Technol. 39 (2004) 3237.

[4] A. Ridha, H. Aderdour, H. Zineddine, M.Z. Benabdallah, Ann. Chim. Sci. Mat. 23 (1998) 161.

[5] S. Aytas, S. Akyil, M.A.A. Aslani, U. Aytekin, J. Radioanal. Nucl. Chem. 240 (1999) 973.

[6] K. Agdi, A. Bouaid, A. M. Esteban, P. F. Hernando, A. Azmani, C. Camara, J. Environ. Monit. 2 (2000) 420.

[7] T.N.C. Dantas, A.A. Dantas Neto, M.C.P.A. Moura, Wat. Res. 35 (2001) 2219.

[8] Y. Al-Degs, M.A.M. Khraisheh, M.F. Tutunji, Wat. Res. 35 (2001) 3724.

[9] R.A. Shawabkeh, M.F. Tutunji, Appl. Clay Sci. 24 (2003) 111.

[10] M.A. Ai-Ghouti, M.A.M. Khraisheh, S.J. Allen, M.N. Ahmad, J. Environ. Manage. 69 (2003) 229.

[11] A.N. Christensen, B. Lundtoft, I.C. Madsen, J. Am. Ceram. Soc. 84 (2001) 878.

[12] E. Alvarez, J. Blanco, P. Avila, C. Knapp, Catal. Today 53 (1999) 557.

[13] Z. Korunic, J. Stored Prod. Res. 34 (1998) 87.

[14] M.K. Hasnuddin Siddiqui, Bleaching Earth, Pergamon Press, Oxford, UK, 1968.

[15] R. Mokaya, W. Jones, M.E. Davies, M.E. Whittle, J. Mater. Chem. 3 (1993) 381.

[16] M.A. Vicente Rodriguez, M. Suarez Barrios, J.D. Lopez Gonzalez, M.A. Banares Munoz, Clays Clay Miner. 42 (1994) 724.

[17] J. Bovey, W. Jones, J. Mater. Chem. 5 (1995) 2027.

[18] P. Kumar, R.V. Jasra, T.S.G. Bhat, Ind. Eng. Chem. Res. 34 (1995) 1440.

[19] P. Komadel, in: P. Misaelides, F. Macasek, T.J. Pinnavaia, C. Colella (Eds.), Natural Microporous Materials in Environmental Technology, Kluwer Academic Pub., Dordrecht, The Netherlands, 1999, p. 3.

[20] H. Kurama, A. Zimmer, W. Reschetilowski, Chem. Eng. Technol. 25 (2002) 301.

[21] A.S. Ozcan, A. Ozcan, J. Colloid Interface Sci. 276 (2004) 39.

[22] W.T. Tsai, K.J. Hsien, J.M. Yang, J. Colloid Interface Sci. 275 (2004) 428.

[23] F. M. Miller, Chemistry: Structure and Dynamics, McGraw-Hill, New York, 1984.

[24] T. E. Hawkinson, D. B. Korpela, in: R.A. Bolmen, Jr. (Ed.), Semiconductor Safety Handbook: Safety and Health in the Semiconductor Industry, Noyes, Westwood, USA, 1997, p. 168.

[25] M. Upfal, C. Doyle, in: R.S. Ratney (Ed.), Hazard Assessment and Control Technology in Semiconductor Manufacturing II, ACGIH, Cincinnati, USA, 1993, p. 121.

[26] W.T. Tsai, K.J. Hsien, C.W. Lai, Ind. Eng. Chem. Res. 43 (2004) 7513.

[27] S. J. Gregg, K. S. W. Sing, Adsorption, Surface Area and Porosity, Second Ed., Academic Press, London, 1982.

[28] J. Aigueperse, in: Ullmann's Encyclopedia of Industrial Chemistry, 6th ed., Vol. 14, Wiley-VCH, Weinheim, Germany, 2003, p. 395.

[29] J.M. Smith, Chemical Engineering Kinetics, 3rd ed., McGraw-Hill, New York, 1981.

[30] J.T. Richardson, Principles of Catalyst Development, Plenum Press, New York, 1989.

[31] S. Lowell, J.E. Shields, Powder Surface Area and Porosity, 3rd ed., Chapman & Hall, London, 1991.

[32] P. Falaras, I. Kovanis, F. Lezou, G. Seiragakis, Clay Miner. 34 (1999) 221.

Table 1

Surface area and porosity of diatomaceous earth (DE)

S_{BET}[a] ($m^2\ g^{-1}$)	S_L[b] ($m^2\ g^{-1}$)	V_t[c] ($cm^3\ g^{-1}$)	ρ_s[d] ($g\ cm^{-3}$)	ρ_p[e] ($g\ cm^{-3}$)	ε_p[f] (-)
3.81 ± 0.01[g]	21.17 ± 0.40	0.0155 ± 0.0009	2.82 ± 0.05	2.70 ± 0.04	0.043 ± 0.004

[a] BET surface area.

[b] Langmuir surface area.

[c] Total pore volume.

[d] True density.

[e] Particle density, calculated by: $\rho_p = 1/[V_t + (1/\rho_s)]$, where ρ_s was determined by pycnometer.

[f] Particle porosity, computed by: $\varepsilon_p = 1 - (\rho_p / \rho_s)$.

[g] Mean ± standard deviation for two determinations.

Table 2

Contents of C, H, N, and Si of DE and modified diatomaceous earths (MDEs) (% oven-dried weight)

Sample ID	C (%)	H (%)	N (%)	Si (%)
DE	0.18	0.33	0.10	41.9
MDE-0.2 N [a]	0.05	0.38	0.14	41.8
MDE-0.5 N [a]	0.02	0.34	0.07	41.5
MDE-1.0 N [a]	0.06	0.22	0.09	41.3
MDE-1.5 N [a]	0.07	0.21	0.05	40.9
MDE-2.5 N [a]	0.04	0.13	0.17	38.8

[a] Prepared in the conditions of temperature of 60 ℃, holding time of 0.5 h, solid/liquid ratio of 5 g/100 g, and various HF concentrations (i.e., 0.2, 0.5, 1.0, 1.5, and 2.5 N).

Table 3

Kinetic parameters for methylene blue adsorption onto DE and MDE-2.5 N [a]

Adsorbent	C_0 (mg dm^{-3})	k (g mg^{-1}min^{-1})	q_e (mg g^{-1})	Correlation coefficient	C_e (mg dm^{-3})
DE	10.1	0.606	2.68	0.999	9.3
	3.9	0.522	1.15	0.999	3.6
	6.1	0.227	2.36	0.999	5.5
MDE-2.5 N [b]	8.0	0.165	2.64	0.999	7.4
	9.7	0.206	2.85	0.998	9.0
	11.9	0.099	4.27	0.997	10.8

[a] Adsorption conditions: adsorbent dosage=0.5 g 2.0 dm^{-3}, agitation speed =400 rpm, pH=7, and temperature = 25 ℃.

[b] MDE-2.5 N: produced from HF concentration=2.5 N, temperature =60 ℃, solid/liquid ratio=5 g/100 g, and time = 30 min.

Table 4

Parameters in the Freundlich isotherm model of MDE-2.5 N at 25 ℃.

K_F [mg g^{-1} (dm^3 mg^{-1})$^{1/n}$]	1/n (-)	R^2
0.32	1.063	0.927

FIGURE CAPTIONS

Figure 1. Effect of HF concentration on BET surface areas of modified diatomaceous earths prepared at the temperatures of 60 and 80 ℃, holding time of 0.5 h and solid/liquid ratio of 5 g/100 mL

Figure 2. Nitrogen adsorption/desorption isotherms of diatomaceous earth (DE) and modified diatomaceous earths (i.e., MDE-1.0 N and MDE-2.5 N).

Figure 3. Pore size distributions of diatomaceous earth (DE) and modified diatomaceous earths (i.e., MDE-1.0 N and MDE-2.5 N) based on BJH desorption *d*A/*d*D pore area.

Figure 4. Effect of temperature on BET surface areas of modified diatomaceous earths prepared at the HF concentration of 2.5 N, holding time of 0.5 h and solid/liquid ratio of 5 g/100 mL

Figure 5. Effect of holding time on BET surface areas of modified diatomaceous earths prepared at the HF concentration of 1.0 N, temperatures of 25-100 ℃ and solid/liquid ratio of 5 g/100 mL

Figure 6. Effect of solid/liquid ratio on BET surface areas of the resulting solid prepared at the HF concentration of 1.0 N, temperature of 80 ℃ and holding time of 0.5 h.

Figure 7. SEM photographs (× 4000) of diatomaceous earth (DE) and modified diatomaceous earth (i.e., MDE-2.5 N).

Figure 8. XRD diffractograms of diatomaceous earth (DE) and modified diatomaceous earths (i.e., MDE-0.2 N, MDE-0.5 N, MDE-1.0 N, MDE-1.5 N and MDE-2.5 N).

Figure 9. FTIR spectra of diatomaceous earth (DE) and modified diatomaceous earths (i.e., MDE-0.2 N, MDE-0.5 N, MDE-1.0 N, MDE-1.5 N and MDE-2.5 N).

Figure 1

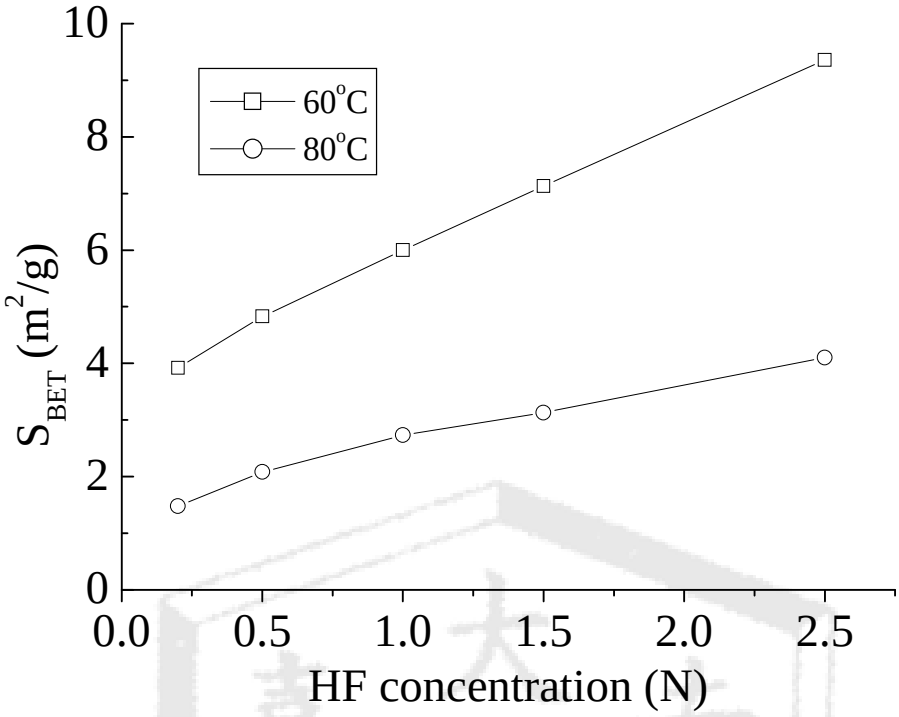

Figure 2

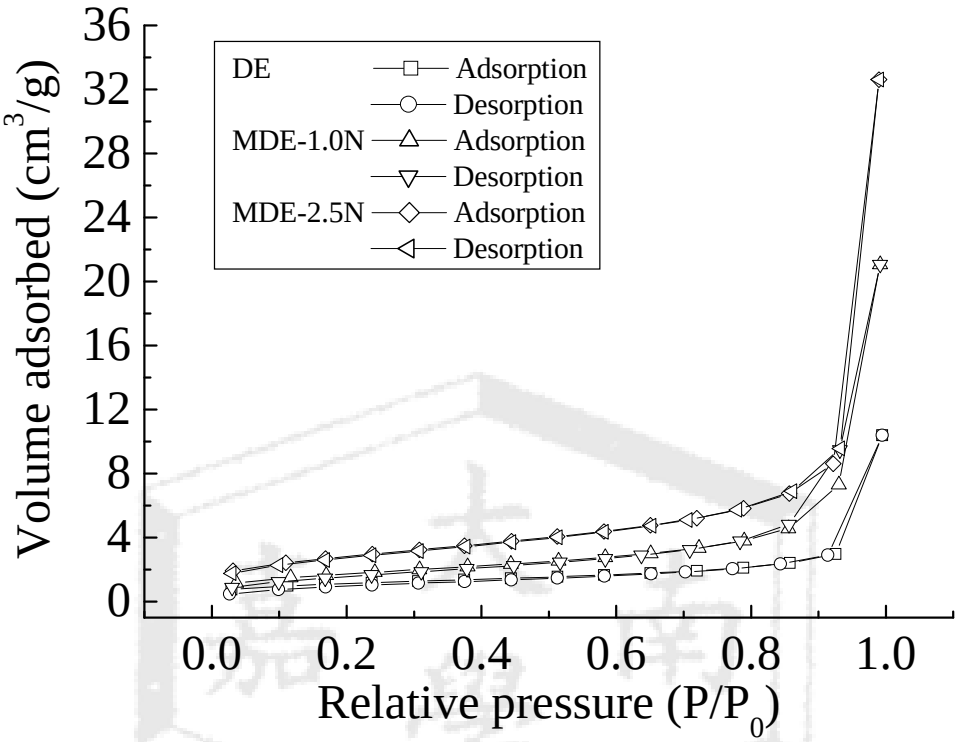
DE
Adsorption
Desorption
MDE-1.0N
Adsorption
Desorption
MDE-2.5N
Adsorption
Desorption
Volume adsorbed (cm3/g)
0
4
8
12
16
20
24
28
32
36
0.0
0.2
0.4
0.6
0.8
1.0
Relative pressure (P/P0)

Figure 3

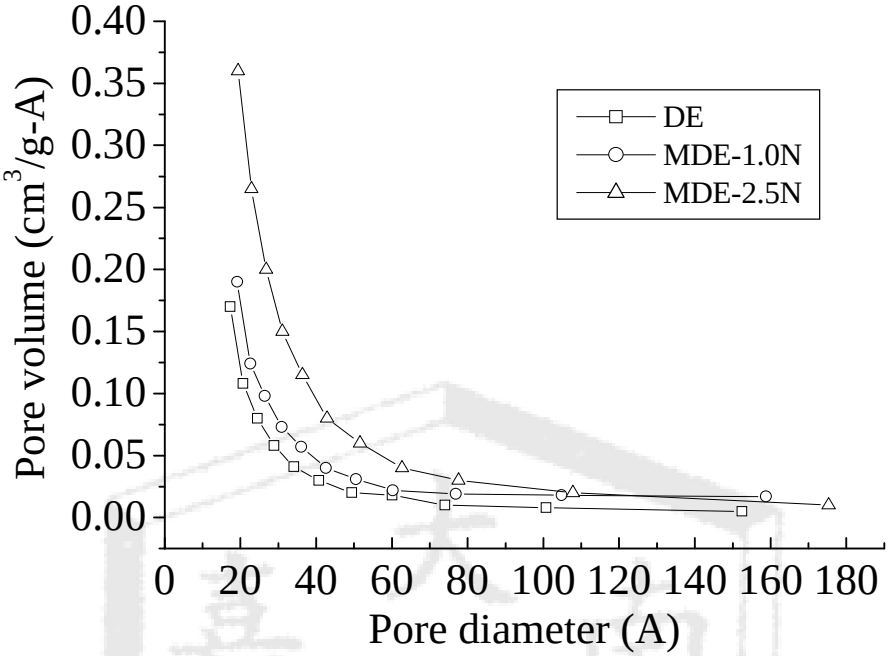
0.40
0.35
0.30
0.25
0.20
0.15
0.10
0.05
0.00
Pore volume (cm3/g-A)
0
20
40
60
80
100
120
140
160
180
Pore diameter (A)
DE
MDE-1.0N
MDE-2.5N

Figure 4

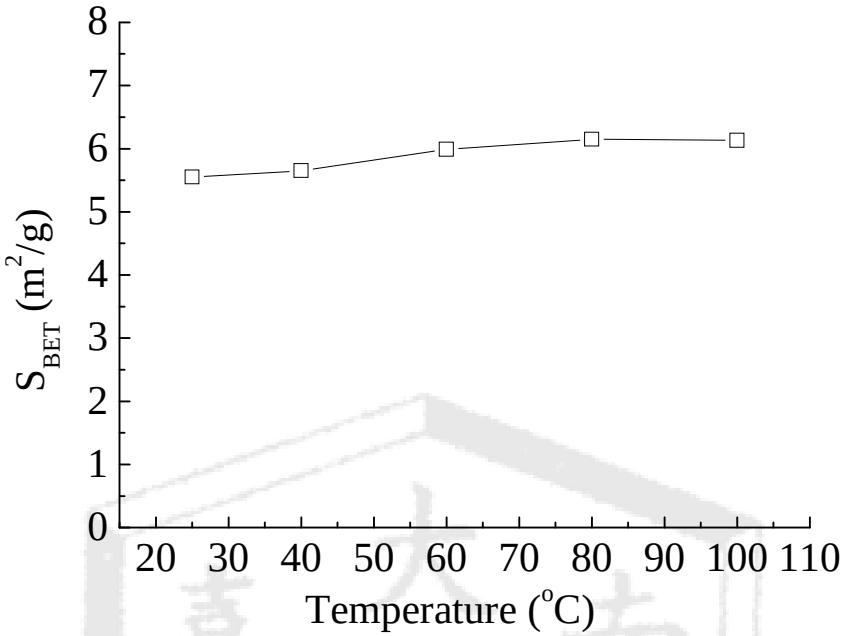
8
7
6
5
4
3
2
1
0
S_{BET} (m^2/g)
20 30 40 50 60 70 80 90 100 110
Temperature (^oC)

Figure 5

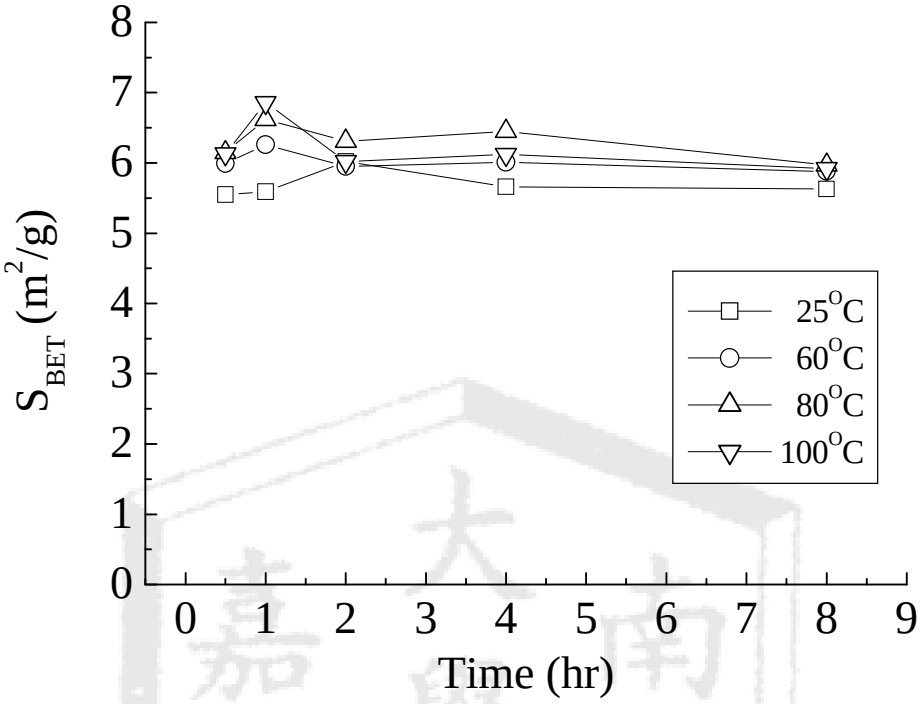

Figure 6

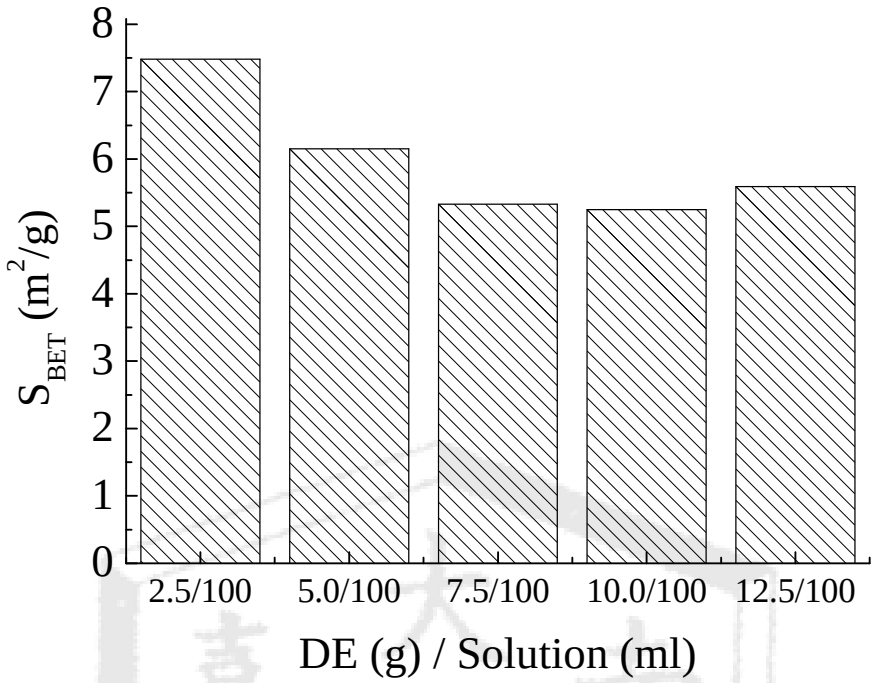
8
7
6
5
4
3
2
1
0
S_{BET} (m^2/g)
2.5/100
5.0/100
7.5/100
10.0/100
12.5/100
DE (g) / Solution (ml)

Figure 7

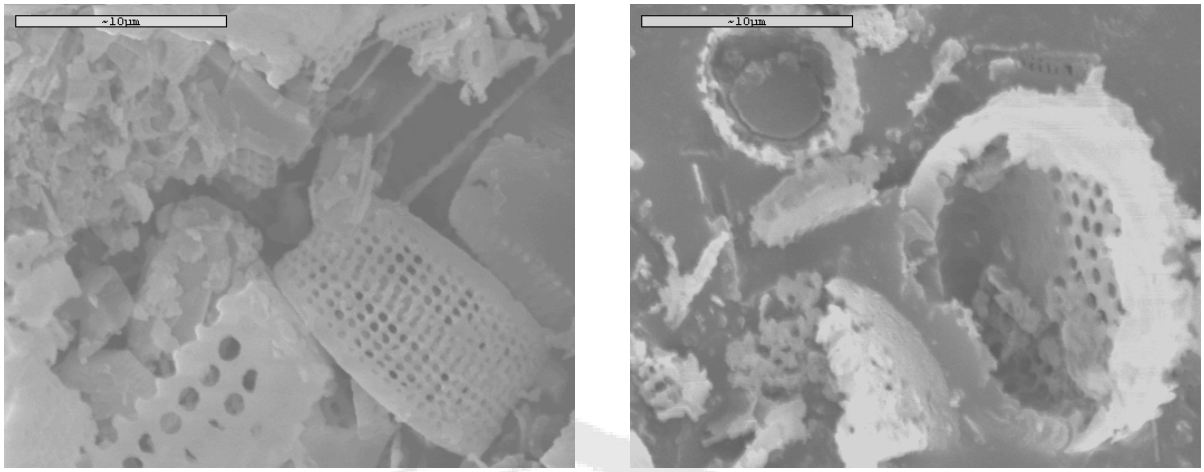

Figure 8

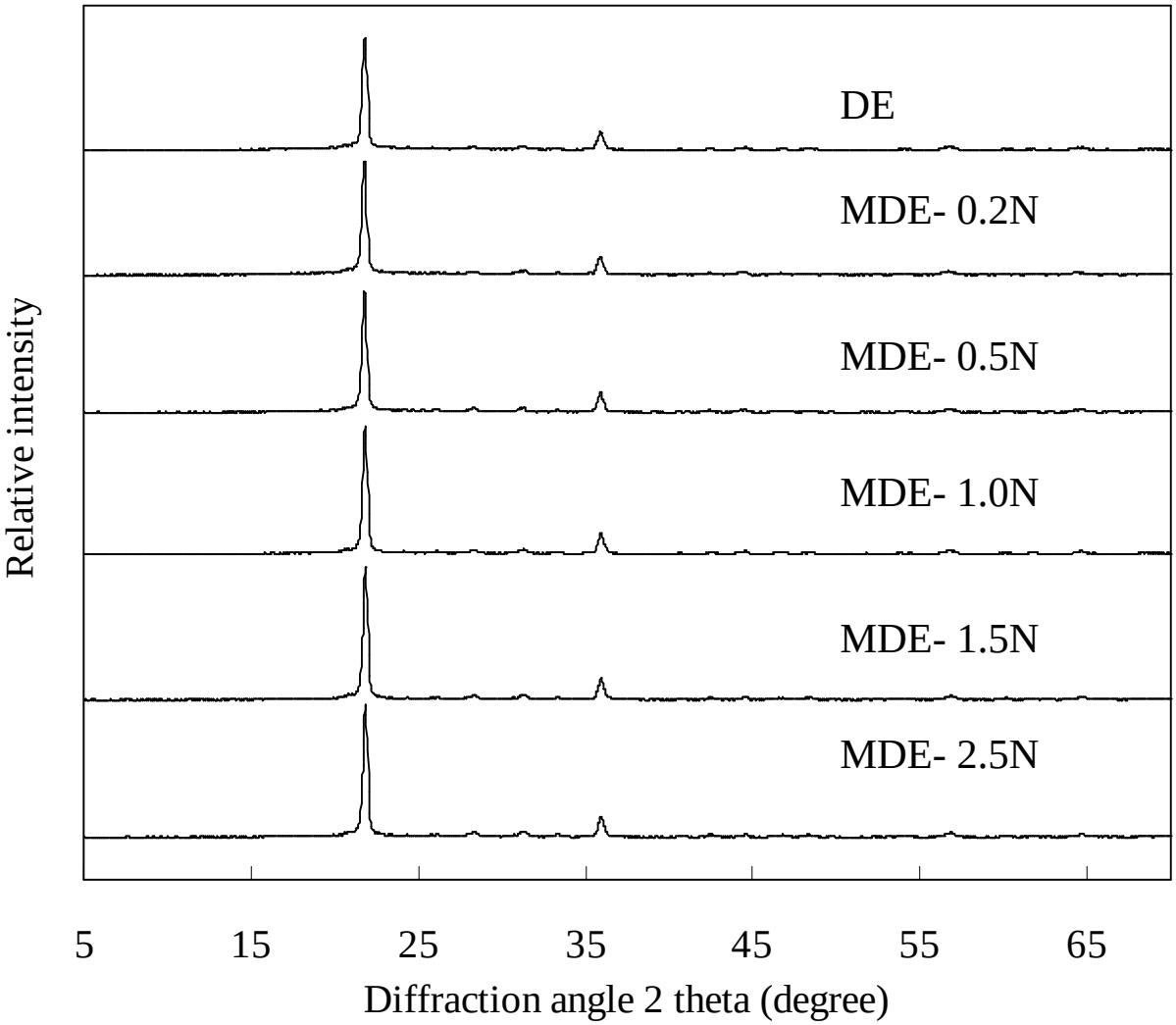
DE
MDE- 0.2N
MDE- 0.5N
MDE- 1.0N
MDE- 1.5N
MDE- 2.5N
Relative intensity
5
15
25
35
45
55
65
Diffraction angle 2 theta (degree)

Figure 9

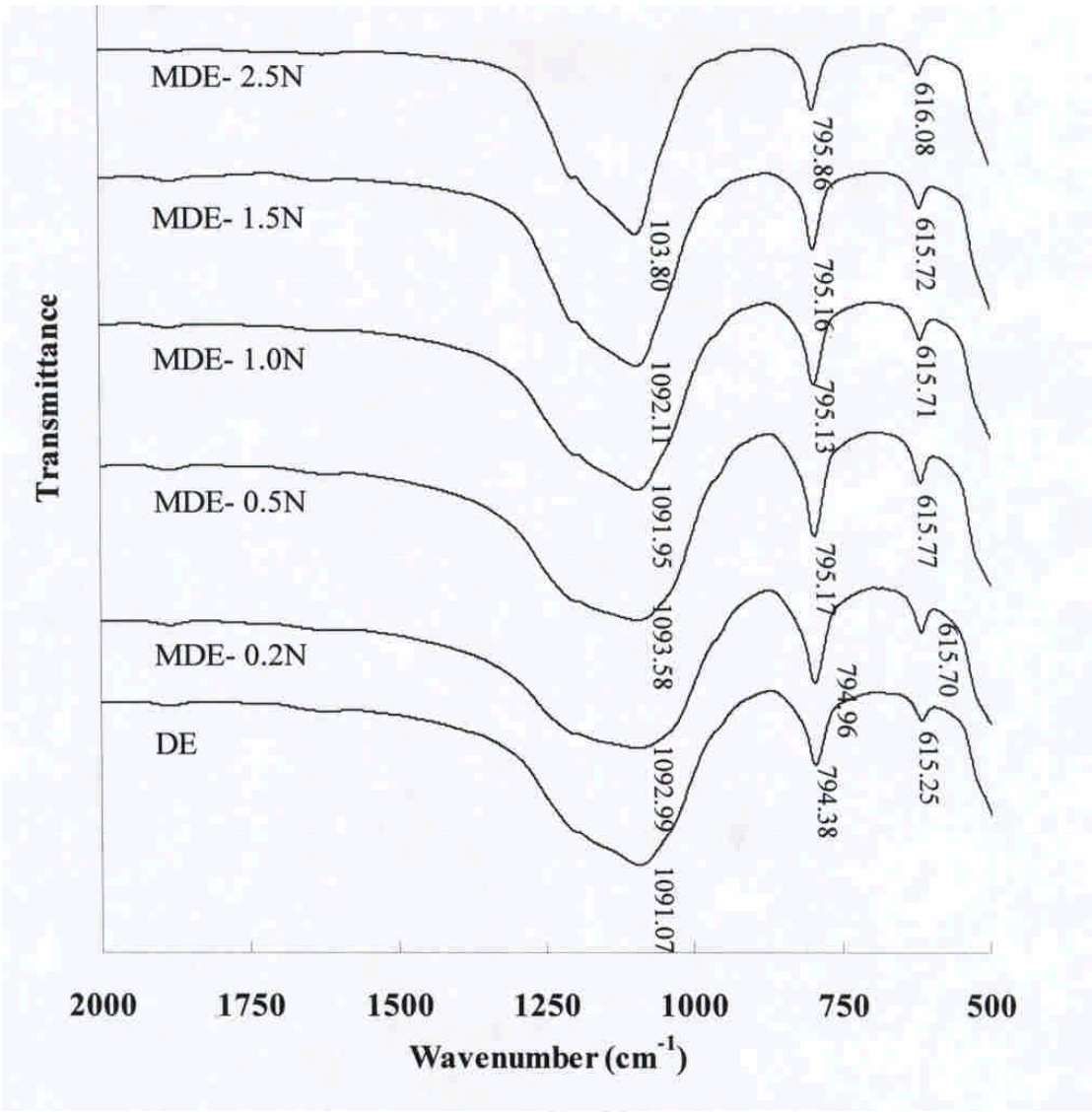
MDE- 2.5N
MDE- 1.5N
MDE- 1.0N
MDE- 0.5N
MDE- 0.2N
DE
616.08
615.72
615.71
615.77
615.70
615.25
795.86
795.16
795.13
795.17
794.96
794.38
1103.80
1092.11
1091.95
1093.58
1092.99
1091.07
Transmittance
2000
1750
1500
1250
1000
750
500
Wavenumber (cm-1)

Ms. Ref. No.: HAZMAT-D-05-00224 (Journal of Hazardous Materials, Accepted)

Adsorption of Bisphenol-A from Aqueous Solution onto Minerals and Carbon Adsorbents

Wen-Tien Tsai *, Chi-Wei Lai, Ting-Yi Su

Department of Environmental Engineering and Science, Chia Nan University of Pharmacy and Science, Tainan 717, Taiwan

Abstract

The adsorption behaviors of bisphenol-A, which has been listed as one of endocrine disrupting chemicals, from aqueous solution onto four minerals including andesite, diatomaceous earth, titanium dioxide, and activated bleaching earth, and two activated carbons with coconut-based and coal-based virgins were examined in this work. Based on the adsorption results at the specified conditions, the adsorption capacities of activated carbons are significantly larger than those of mineral adsorbents, implying that the former is effective for removal of the highly hydrophobic adsorbate from the aqueous solution because of its high surface area and low surface polarity. The adsorption capacities of bisphenol-A onto these mineral adsorbents with different pore properties are almost similar in magnitude mainly due to the weakly electrostatic interaction between the mineral surface with negative charge and the target adsorbate with hydrophobic nature. Further, a simplified kinetic model, pseudo-second-order, was tested to investigate the adsorption behaviors of bisphenol-A onto the two common activated carbons at different solution conditions. It was found that the adsorption process can be well described with the pseudo-second- order model. The kinetic parameters of the model obtained in the present work are in line with the pore properties of the two adsorbents.

Keywords: Bisphenol-A; Adsorption; Activated carbon; Mineral adsorbent; Kinetic modeling

---

* Corresponding author: Tel.: +886-6-2660393; Fax: +886-6-2669090.
E-mail address: wwtsai@mail.chna.edu.tw

1. Introduction

In recent years, the environmental pollution of endocrine disrupting chemicals (EDCs) in water sources and factory effluents has aroused the public concerns. Among these anthropogenic chemicals, bisphenol-A, which has been listed as one of EDCs [1], is widely used in the plastic industry as a monomer for the production of polycarbonate and epoxy resin [2]. Its annual production capacity in Taiwan has now exceeded 390,000 metric tons in response to the increasing needs in the compact discs and construction materials [3]. As expected, its environmental distribution will be highly widespread. Because of its reported threats to human health and reproductive biology [4], an environmental technoloy for the rapid removal of bisphenol-A from the water body is required.

Conventional methods for the removal of organic pollutants in effluents may be divided into three main categories: physical, chemical, and biological [5]. Among them, physical adsorption is generally considered to be an effective method for quickly lowering the concentrations of organic molecules in an effluent because common adsorbents including mineral clay and activated carbon generally possess large accessible internal surface and/or external surface. It is well known that the unique surface property of activated carbon, in contrast to the other non-carbon adsorbents (e.g., clay), is that its surface is non-polar or only slightly polar [6]. In this regard, activated carbon is now the most widely used adsorbent for removal of organic molecules. However, the published information on the adsorption of bisphenol-A onto mineral and carbon adsorbents is limited. Nakanish *et al.* [7] investigated the adsorption characteristics of bisphenol-A onto the carbonaceous adsorbents produced from a variety of wood chips. Based on the adsorption isotherms at 25 ℃ onto the carbonaceous materials by the Freundlich model, the results indicated that the affinity between bisphenol-A and the carbonaceous material was similar. Asada *et al.* [8] pointed out that porous carbon produced from the carbonization of bamboo could be used as an effective adsorbent for removal of bisphenol-A from the aqueous solution. According to the results from the adsorption isotherm, the adsorption amount of bisphenol-A increased as the carbonization temperature increased, which is in line with the corresponding BET surface area. They also found that carbon adsorbent with a low surface polarity will be more effective for the adsorption of a high hydrophobic substance like bisphenol-A. Choi *et al.* [9] examined the removal performances of three endocrine disrupting chemicals (e.g., bisphenol-A) using activated carbons with three different base materials in the column test, showing that bisphenol-A can be effectively adsorbed onto all carbons, and the pore volume was found more significant to adsorption capacity than the specific surface area based on the adsorption isotherm, but the surface charge was also profound probably due to the electrical

interaction between the nearly non-polar carbon surface and highly hydrophobic molecule. Bautista-Toledo *et al.* [10] studied the adsorption of bisphenol-A from water on activated carbon, showing that the system fundamentally depends on the chemical nature of the carbon surface and the pH of the solution. The presence of mineral mater in carbons reduces their adsorption capacity because of the hydrophilic nature of the matter.

With respect to the adsorption characteristics of bisphenol-A in the aqueous solution onto the mineral materials, and the adsorption kinetics and its modeling in the case of the activated carbon, the information is scarce. Thus, the objectives of this work were to (1) determine the extent of the adsorption of bisphenol-A onto various minerals and activated carbons at the specified conditions, (2) evaluate the usefulness of pseudo-second order model for analyzing the adsorption system between the hydrophobic adsorbate and the carbon adsorbent, and (3) investigate the applicability of common isotherm models (i.e., Langmuir & Freundlich) based on the adsorption capacities from the fittings of the adsorption rate model.

2. Methods

2.1. Materials

The endocrine disrupting chemicals used as target adsorbate in the present study is bisphenol-A (99+% purity), which was purchased from Aldrich Chemical Co. (Milwaukee, U.S.A.). Its CAS identification information and molecular weight are 80-05-7 and 228.29 g/mol, respectively. The molecular structure of this adsorbate is shown in Fig. 1. Two different kinds of the materials were used as adsorbents, including minerals and activated carbons. The former included andesite from local clay manufacturer (Taitung, Taiwan) with the particle size of ＜0.074 mm (＜mesh No. 200), diatomaceous earth from Celite Co. (Santa Barbara, USA) with the Product Grade 577 [11], titanium dioxide (photocatalyst P-25) from Degussa AG Co. (Frankfurt, Germany) with 80% anatase, 20% rutile and BET area of about 50 m^2 g^{-1}), and activated bleaching earth from Mizusawa Co. (Tokyo, Japan) with the main components of 75.8 % SiO_2, 8.8 % Al_2O_3 and 3.0 % Fe_2O_3 [12]. The later were two different kinds of the commercial granular activated carbons from Calgon Carbon Co. (Pittsburgh, USA) with the notations of PCB (coconut shell-based) and BPL (bituminous coal-based), respectively. The activated carbons were ground and sieved to mesh No. ranges of 60-120 (0.125 - 0.250 mm), 120-200 (0.074 - 0.125 mm), and ＜200 (＜0.074 mm). These adsorbents were dried at about 100 ℃ and then stored in a desiccator, before being used in the analytical measurements and adsorption experiments. The main pore properties of these adsorbents using an automated nitrogen adsorption/desorption analyzer (Model No.: ASAP 2010; Micromeritics Co.; Atlanta, USA) are given in Table 1. H_2SO_4 and NaOH were used for adjusting initial pH value of

aqueous solution to obtain the extent of the adsorption of bisphenol-A.

2.2. Adsorption studies

All the experiments of adsorption kinetics were carried out in a *ca.* 3-dm^3 stirred batch adsorption apparatus with four baffles as similarly described in our previous studies [11-16]. All the bisphenol-A solutions were prepared with de-ionized water. The effect of agitation speed at 200, 400 and 600 rpm on the adsorption uptake was first tested and depicted in Fig. 2, showing that it seemed to be negligible. The adsorption uptake of the adsorbents under the initial bisphenol-A concentration of 60 mg dm^{-3}, mixing rate of 400 rpm, temperature of 25 ℃, pH of 7.0 and dosage of 0.5 g 2.0 dm^{-3} was first investigated for the purpose of studying the effectiveness of adsorbents. From the results in Table 2, it was found that the adsorption capacities of activated carbons are significantly superior to those of the minerals at the same conditions. Thus, the activated carbons were further used to study the variation of adsorption at various initial bisphenol-A concentrations (i.e., 60-100 mg dm^{-3}), pH (i.e., 3-11), adsorbent dosage (i.e., 0.05-0.25 g dm^{-3}), and adsorbent size (i.e., ＜0.074, 0.074 - 0.125, and 0.125 – 0.250 mm). The solution sample (about 10 cm^3) was taken at specified time up to 2 hours and then filtrated with fiber membrane (Cat. No.: A045A025A; ADVANTEC MFS, Inc.). The bisphenol-A concentration analysis of filtrate solution was immediately measured with UV/Visible spectrophotometer (Model: U-2001; Hitachi Co., Japan) at a 221 nm wavelength [7]. The amount of bisphenol-A adsorbed (q_t, mg g^{-1}) was determined as follows:

$$q_t = (C_o - C_t) \cdot V/m \qquad (1)$$

where C_o and C_t are the initial and liquid-phase concentrations of the bisphenol-A solution at t time (mg dm^{-3}), respectively, V is the volume (*ca.* 2.0 dm^3) of aqueous solution containing bisphenol-A, and m is the mass of dry adsorbent used (g). In order to evaluate the statistical significance of data in the kinetic experiments, a preliminary experiment was also repeated under identical conditions, showing that the reproducibility of the measurements is within 5 % in the adsorption experiments.

3. Adsorption kinetic model

The adsorption process in a stirring chamber generally involves several transport stages [6]; i.e., external diffusion, internal diffusion and actual adsorption process. The model of the separation process should adequately account for the mass balance and the adsorption equilibrium if the system is isothermal. In most cases, the resistance to internal diffusion can be significant. However, the local rate of adsorption is assumed to be relatively fast and the

resistance to external diffusion is experimentally controlled to be negligible, compared to the intra-particle diffusion. Although many theoretical model equations have been proposed for describing the adsorption kinetics based on mass balance, pore diffusion rate and initial/boundary conditions. These equations are not only complicated and impractical while using them, but also require detailed data such as the characteristics of adsorbate and adsorbent.

In order to investigate the adsorption characteristics of bisphenol-A onto minerals and activated carbons, the pseudo-second order kinetics model was used to test the adsorption dynamics in this work because of its good applicability in most cases in comparison with pseudo-first order model and intra-particle diffusion model [17-20]:

$$d\,q_t/d\,t = k.\,(q_e - q_t)^2 \qquad (2)$$

where k is the pseudo-second order rate constant (g mg^{-1} min^{-1}), q_e is the amount of bisphenol-A adsorbed at equilibrium (mg g^{-1}), q_t is the amount of bisphenol-A adsorbed at time t (mg g^{-1}). Integrating Eq. (2) for the boundary conditions $t = 0$ to $t = t$ and $q_t = 0$ to $q_t = q_t$, gives:

$$1/(q_e - q_t) = 1/q_e + k.\,t \qquad (3)$$

Eq. (3) can be rearranged to obtain a linear form of :

$$t/q_t = 1/(k.\,q_e^{\,2}) + (1/q_e).\,t \qquad (4)$$

Rate parameters, k and q_e, can be directly obtained from the intercept and slope of the plot of (t/q_t) against t. The equilibrium concentration (i.e., C_e) can be further determined by the mass balance principle as the value of q_e has been obtained from the fitting of Eq. (4). Also, half of the adsorption time, $t_{1/2}$, is the time required for the adsorbent to take up half as much paraquat as it will at equilibrium (i.e., $t = t_{1/2}$ as $q_t = q_e/2$). This period of time is often used as a measure of the rate of adsorption and is given from the rearrangement of Eq. (3) as follows:

$$t_{1/2} = 1/(k.\,q_e) \qquad (4)$$

On the other hand, the initial adsorption rate, h, can be further obtained using Eq. (2) at the initial adsorption time (i.e., $t = 0$ as $q_t = 0$) as the value of q_e has been determined from the fitting of Eq. (3) as follows:

$$h = k.\,q_e^{\,2} \qquad (5)$$

The equilibrium concentration (i.e., C_e) can be further calculated from Eq.(1) as the value of q_e has been obtained from the fitting of Eq.(3) as follows.

$$C_e = C_o - q_e\,.\,m/V \qquad (6)$$

In the present study the effects of the initial bisphenol-A concentration, pH, adsorbent mass, and particle size on the rate and extent of adsorption were presented and discussed as below.

4. Results and discussion

4.1 Adsorption characteristics of bisphenol-A onto minerals and activated carbons

Adsorption studies of bisphenol-A onto minerals and activated carbons were carried out at initial concentration of 20 g dm^{-3}, adsorbent dosage of 0.5 g 2.0 dm^{-3}, agitation rate of 400 rpm, pH of 7.0, adsorption time of 2 hours, and temperature of 25 ℃. Table 2 lists the results of adsorption kinetics of each adsorbent using the fittings of pseudo-second order model. Several noteworthy features may be obtained from the results shown in Table 2.

1. Using the regression analysis (least square method), the model obviously appears to fit the experimental adsorption data reasonably well
2. The adsorption capacities of bisphenol-A onto mineral adsorbents (i.e., andesite, diatomaceous earth, titanium dioxide, and activated bleaching earth) are significantly smaller than those of carbon adsorbents (i.e., BPL and PCB) showing that carbon adsorbent with a low surface polarity will be more effective than mineral adsorbent for the adsorption of bisphenol-A since it has a high value (i.e., 3.1) of octanol-water partition coefficient (K_{ow}) and thus possesses a highly hydrophobic property [9].
3. It was observed that the adsorption capacities of bisphenol-A below 1 mg g^{-1} were obtained for all mineral adsorbents, not in proportion to their pore properties listed in Table 1. It revealed that the pore volume and/or particle surface area in the cases of these mineral adsorbents are not determining factors for the removal of bisphenol-A from the aqueous solution probably due to the repulsive interaction between the mineral surface with negative charge and the target adsorbate with hydrophobic structure.
4. It was observed that the total amount of the acidic groups of carbon-BPL is larger than that of carbon-PCB as studied previously [24]. Therefore, the pore property of carbon-BPL is slightly superior to that of carbon-PCB but the qe of carbon-PCB is exactly same as that of carbon-BPL due to the electrostatic repulsion between the bisphenol-A and the negatively charged surface as a result of organic functional groups containing oxygen.
5. Consequently, the initial adsorption rates of carbon adsorbents are more rapid than those of mineral adsorbents. In other words, the activated carbon adsorbs more nonpolar and weakly polar organic molecules than mineral adsorbents do [6].

From the results described above, the most significant factors in determining adsorption capacity are not only the physical characteristics of adsorbents including pore volume and surface area but also their chemical characterizations (i.e., surface polarity). Although the activated bleaching earth possesses a mesoporous structure with high BET surface area of *ca.* 260 m^2/g, for

example, its adsorption capacity (0.88 mg/g) for bisphenol-A is so low in comparison with those (0.53 and 0.73 mg/g, respectively) of other mineral adsorbents (i.e., andesite and diatomaceous earth) with low BET surface areas (*ca.* 3 and 4 m^2/g, respectively) as a result of electrostatic repulsion between the negatively charged surface and hydrophobis adsorbate (i.e., bisphenol-A). As expected, the activated carbon could adsorb significant quantity of bisphenol-A because of its large accessible internal surface (*ca.*1000 m^2/g) and its very low polarity in the surface.

4.2 Adsorption kinetics of bisphenol-A onto activated carbon

4.2.1. Effect of initial concentration

The adsorption uptake and its kinetics using pseudo-second order kinetics model at different initial bisphenol-A concentrations onto the activated carbons BPL and PCB are presented in Table 3. As seen from Table 3, it is evident that the kinetic modeling of the bisphenol-A adsorption onto the carbon adsorbent well follows this model with the correlation coefficients of higher than 0.999 for all the system in the present work. The equilibrium adsorption capacity (i.e., q_e) increased as the initial bisphenol-A concentration (i.e., C_0) increased from 60 to 100 mg dm^{-3}, showing that the initial concentration provides an powerful driving force to overcome the mass transfer resistance between the aqueous and solid phases [22]. As expected from the results in Table 1, the maximum loading capacities of the activated carbon BPL were higher than those of the activated carbon PCB. For example, 357.1 mg g^{-1} for the activated carbon BPL, and 270.3 mg g^{-1} for the activated carbon PCB at 100 mg dm^{-3} initial bisphenol-A concentration. Further, it was found that the variations of rate constant (i.e., k) seem to have a decreasing trend with initial bisphenol-A concentration increased, which is consistent with similar studies [16, 18, 19, 22].

4.2.2. Effect of initial pH

Using the fittings of pseudo-second order kinetics model, the variations of equilibrium adsorption capacities of both carbon adsorbents with initial pH are given in Table 4. Again, the kinetics of the adsorption follows this model with the regression coefficients of higher than 0.999, as listed in Table 4. Obviously, the adsorption capacity (i.e., q_e) exhibits a constant extent as the pH was increased from 3 to 9, while the bisphenol-A adsorption shows a decreasing trend at a higher pH ranging from 9 to 11. These results are consistent with those studied by Bautista-Toledo *et al.* [10]. The result could be attributed to the pka value of bisphenol-A ranging 9.6-10.2 [23], implying that the ionization of bisphenol-A occurred at around pH 9-10 to form the bisphenolate anion. Therefore, the reduction in the adsorption capacity of the activated carbons at very basic pH range ($>$ 10.0) may be probably due to the electrostatic repulsion

between the bisphenolate anion from the ionization of bisphenol-A and the slightly negatively charged surface as a result of organic functional groups containing oxygen [24].

4.2.3. Effect of adsorbent dosage

The effect of varying the activated carbon mass on bisphenol-A adsorption at the initial concentration of 60 mg dm^{-3}, pH of 7.0, agitation rate of 400 rpm, particle size of ＜0.074 mm, and temperature of 25 ℃ has been carried out. The values of parameters for the adsorption system are listed in Table 5. Evidently, the correlation between the experimental and theoretical results is also good. As expected, the bisphenol-A concentration in the solution rapidly decreased and the rate constant, k, thus increased at a larger value as the adsorbent dosage increased. This implies that the number of adsorption sites increases in parallel with increasing adsorbent dosage. But the adsorption capacity (i.e., q_e) decreased as the adsorbent dosage increased. Such a phenomenon is similar to those of Ho & Chiang [19] and Hue et al. [25] for the adsorption of dye onto activated clay. This leads to make a suggestion that, in order to obtain the optimal adsorbent dosage, higher initial bisphenol-A concentrations should be tested in conjunction with appropriate adsorbent dosage [18].

4.2.4. Effect of adsorbent size

The effect of varying the activated carbon particle size on bisphenol-A adsorption has been investigated, and the results are listed in Table 6. It can be seen that the adsorption capacity (i.e., q_e) of the activated carbon BPL decreased from 238.0 to 137.0 mg g^{-1} as the adsorbent particle size increased from 0-0.074 to 0.125-0.250 mm, while in the case of the activated carbon PCB, the adsorption capacity decreased from 227.3 to 80.0 mg g^{-1}. This behavior can demonstrate that larger surface area of adsorbent particle for a given mass of activated carbon is associated with smaller particle size [13, 19, 25], resulting in the adsorption availability increased. The results obtained from this section of experiments also indicated that the rate constant (k) seemed to be significantly decreased as the adsorbent size increased from 0-0.074 to 0.074-0.125 mm.

4.3. Adsorption isotherm

Two common isotherm equations have been applied to model the isotherms in the present study: the Langmuir and Freundlich models [26, 27].

Langmuir : $$1/q_e = 1/[(K_L \cdot q_m)\, C_e] + 1/q_m \quad (7)$$

Freundlich : $$q_e = K_F \cdot C_e^{1/n} \quad (8)$$

In Eq. (7), C_e and q_e are the concentration (mg dm^{-3}) and amount (mg g^{-1}) of bisphenol-A adsorbed at equilibrium, respectively, K_L is a direct measure of the intensity of the adsorption

process (dm^3 mg^{-1}), and q_m is a constant relating to the surface area occupied by a monolayer of adsorbate, reflecting the adsorption capacity (mg g^{-1}). Based on the data of q_e from the fittings of the pseudo-second order adsorption rate model, q_m and K_L can be determined from its slope and intercept from a typical plot of $1/q_e$ vs. $1/C_e$. In Eq. (8), K_F is a constant for the system, related to the bonding energy. K_F can be defined as adsorption or distribution coefficient and represents the general capacity of bisphenol-A adsorbed onto adsorbents for a unit equilibrium concentration (i.e., $C_e = 1$ mg dm^{-3}). The slope 1/n, ranging between 0 and 1, is a measure for the adsorption intensity or surface heterogeneity.

The results of the Langmuir and Freundlich isotherms fitted by using the data of adsorption capacity from the regression of Eq. (2) at 25 ℃ are presented in Table 7. Obviously, it can be seen in Fig. 3 that the Freundlich model yields a somewhat better fit than the Langmuir model [7, 8], as reflected with correlation coefficients (R^2) of 0.951 vs. 0.770 and 0.963 vs. 0.854 for the activated carbons BPL and PCB, respectively. It has been known that the magnitudes of K_L and K_F indicate a measure of the adsorbent capacity. As indicated in Table 7, the values of K_L and K_F of adsorbent BPL are larger than those of adsorbent PCB. This is consistent with the results based on their pore properties in Table 1. The adsorption isotherms revealed that the activated carbon can uptake over 200 mg g^{-1} in relatively low concentration of the bisphenol-A in aqueous medium. As also illustrated in Table 7, the values of 1/n are significantly less than unity indicating a favorable adsorption system.

5. Conclusions

The uses of minerals and carbon adsorbents for the adsorption of bisphenol-A from aqueous solution have been examined. The results showed that the adsorption capacities of bisphenol-A onto mineral adsorbents are significantly smaller than those of carbon adsorbents. It seemed that carbon adsorbent with a low surface polarity will be more effective than mineral adsorbent for the removal of the hydrophobic adsorbate from the aqueous solution. Furthermore, the adsorption kinetics of bisphenol-A onto the activated carbon can be well described by pseudo-second order reaction model. The kinetic parameters thus obtained from the fittings of the model were dependent on initial adsorbate concentration, pH, adsorbent dosage and adsorbent particle size. From the isotherm data obtained from the fittings of the pseudo-second order model, the Freundlich model yields a somewhat better fit than the Langmuir model in the adsorption of bisphenol-A onto activated carbon.

Acknowledgements

This research was supported by NSC (National Science Council, Taiwan) under contract number NSC 93-2211-E-041-008.

References

[1] C.M. Markey, C.L. Michaelson, C. Sonnenschein, A.M. Soto, Alkylphenols and bisphenol-A as environmental estrogens, in: M. Metzler (Ed.), The Handbook of Environmental Chemistry, Vol. 3, Part L (Endocrine Disruptors, Part I), Springer-Verlag, Berlin, Germany, 2001, p.129-153.

[2] C.A. Staples, P.B. Dorn, G.M. Klecka, S.T. O'Block, L.R. Harris, A Review of the environmental fate, effects, and exposures of Bisphenol-A, Chemosphere 36 (1998) 2149-2173.

[3] C.S. Torng, Important reports in the 2004 on chemical industry in Taiwan, Chem. Eng. (in Chin.) 52(3) (2005) 66-77.

[4] M.Y. Chen, M. Ike, M. Fujita, Acute toxicity, mutagenicity, and estrogenicity of bisphenol-A and other bisphenols, Environ. Toxicol. 17 (2002) 80-86.

[5] O.J. Hao, H. Kim, P.C. Chiang, Decolorization of wastewater, Crit. Rev. Environ. Sci. Technol. 30 (2000) 449-505.

[6] R.T. Yang, Gas Separation by Adsorption Processes, Butterworths, Boston, Mass., 1987.

[7] A. Nakanishi, M. Tamai, N. Kawasaki, T. Nakamura, S. Tanada, Adsorption characteristics of bisphenol a onto carbonaceous materials produced from wood chips as organic waste, J. Colloid Interface Sci. 252 (2002) 393-396.

[8] T. Asada, K. Oikawa, K. Kawata, S. Ishihara, T. Iyobe, Study of removal effect of bisphenol-A and β - estradiol by porous carbon, J. Health Sci. 50 (2004) 588-593.

[9] K.J. Choi, S.G. Kim, C.W. Kim, S.H. Kim, Effects of activated carbon types and service life on removal of endocrine disrupting chemicals: amitrol, nonylphenol, and bisphenol-A, Chemosphere 58 (2005) 1535-1545.

[10] I. Bautista-Toledo, M.A. Ferro-Garcia, C. Moreno-Castilla, F.J. Vegas Fernandez, Bisphenol-A removal from water by activated carbon. Effects of carbon characteristics and solution chemistry, Environ. Sci. Technol. 39 (2005) 6246-6250.

[11] W.T. Tsai, K.J. Hsien, J.M. Yang, Silica adsorbent prepared from spent diatomaceous earth and its application for removal of dye from aqueous solution, J. Colloid Interface Sci. 275 (2004) 428-433.

[12] W.T. Tsai, C.W. Lai, K.J. Hsien, The effect of pH and salinity on kinetics of paraquat sorption onto activated clay, Colloid Surf. (A) 224 (2003) 99-105.

[13] W.T. Tsai, C.W. Lai, K.J. Hsien, Effect of particle size of activated clay on the adsorption of paraquat from aqueous solution, J. Colloid Interface Sci. 263 (2003) 29-34.

[14] W.T. Tsai, C.W. Lai, K.J. Hsien, Adsorption kinetics of herbocide paraquat from aqueous solution onto activated bleaching earth, Chemosphere 55 (2004) 829-837.

[15] W.T. Tsai, K.J. Hsien, Y.M. Chang, C.C. Lo, Removal of herbicide paraquat from aqueous solution by adsorption onto spent and treated diatomaceous earths, Bioresource Technol. 96 (2005) 657-663.

[16] W.T. Tsai, Y.M. Chang, C.W. Lai, C.C. Lo, Adsorption of Basic Dyes in Aqueous Solution by Clay Adsorbent from Spent Bleaching Earth, Appl. Clay Sci. 29 (2005) 149-154.

[17] Y.S. Ho, G. McKay, The kinetics of sorption of divalent metal ions onto sphagnum moss peat, Water Res. 34 (2000) 735-742.

[18] Y.S. Ho, C.C. Chiang, Y.C. Hsu, Sorption kinetics for dye removal from aqueous solution

using activated clay, Sep. Sci. Technol. 36 (2001) 2473-2488.

[19] Y.S. Ho, C.C. Chiang, Sorption studies of acid dye by mixed sorbents, Adsorption 7 (2001) 139-147.

[20] F.C. Wu, R.L. Tseng, R.S. Juang, Kinetic modeling of liquid-phase adsorption of reactive dyes and metal ions on chitosan, Water Res. 35 (2001) 613-618.

[21] Z. Aksu, J. Yener, A comparative adsorption/biosorption study of mono-chlorinated phenols onto various sorbents, Waste Manage. 21 (2001) 695-702.

[22] W.T. Tsai, C.Y. Chang, C.H. Ing, C.F. Chang, Adsorption of Acid Dyes from Aqueous Solution on Activated Bleaching Earth, J. Colloid Interface Sci. 275 (2004) 72-78.

[23] Y. Yoon, P. Westerhoff, S.A. Snyder, M. Esparza, HPLC-fluorescence detection and adsorption of bisphenol-A, 17β-estradiol, and 17α-ethynyl estradiol on powdered activated carbon, Water Res. 37 (2003) 3530-3537.

[24] W.T. Tsai, C.Y. Chang, Surface characterization and thermodynamics of adsorption of methylene chloride on activated carbons, J. Environ. Sci. Health A30 (1995) 525-535.

[25] Y.C. Hsu, C.C. Chiang, M.F. Yu, Adsorption behaviors of basic dyes on activated clay, Sep. Sci. Technol. 32 (1997) 2513-2534.

[26] B. Al Duri, in: G. McKay (Ed.), Use of Adsorbents for the Removal of Pollutants from Wastewaters, CRC Press, Boca Raton, Fla., 1996.

[27] K.E. Noll, V. Gounaris, W.S. Hou, Adsorption Technology for Air and Water Pollution Control, Lewis, Chelsea, Mich.,1992.

Table 1
Main physical properties of minerals and activated carbons used as adsorbents in the present study [a]

Sample	S_{BET} [b] (m^2 g^{-1})	S_L [c] (m^2 g^{-1})	V_t [d] (cm^3 g^{-1})
Andesite [a]	2.7	17.1	0.0098
Diatomaceous earth	3.8	21.2	0.0155
Titanium dioxide	50.1	408	0.247
Activated bleaching earth	257	388	0.374
Activated carbon- PCB [a]	916	1606	0.576
Activated carbon- BPL [a]	1060	1958	0.714

[a] Particle size is less than 0.074 mm.
[b] BET surface area.
[c] Langmuir surface area.
[d] Total pore volume.

Table 2

Pseudo-second order parameters for the adsorption of bisphenol-A onto the minerals and activated carbons [a]

Sample	k (g mg^{-1}min^{-1})	q_e (mg g^{-1})	$t_{1/2}$ (min)	h (mg g^{-1}min^{-1})	C_e (g dm^{-3})	R^2
Andesite	12.00	0.53	0.16	3.36	19.87	1.000
Diatomaceous earth	7.46	0.73	0.18	3.95	19.82	1.000
Titanium dioxide	48.01	0.33	0.06	5.23	19.92	1.000
Activated bleaching earth	4.02	0.86	0.29	2.98	19.78	1.000
Activated carbon- PCB	0.08	78.13	0.16	476	0.47	1.000
Activated carbon- BPL	0.23	78.13	0.05	1429	0.47	1.000

[a] Adsorption conditions: initial concentration = 20 g dm^{-3}, adsorbent dosage = 0.5 g 2.0 dm^{-3}, agitation rate = 400 rpm, pH = 7.0, and temperature = 25 ℃.

Table 3

Pseudo-second order parameters for the adsorption of bisphenol-A onto the activated carbons at various initial concentrations [a]

Activated carbon	Initial concentration (mg dm^{-3})	Pseudo-second order		
		k (g $mg^{-1}min^{-1}$)	q_e (mg g^{-1})	R^2
BPL	60	10.25×10^{-3}	238.0	1.000
	70	5.95×10^{-3}	270.3	1.000
	80	4.36×10^{-3}	303.0	1.000
	90	3.21×10^{-3}	333.3	1.000
	100	2.70×10^{-3}	357.1	0.999
PCB	60	3.28×10^{-3}	227.3	0.999
	70	2.21×10^{-3}	243.9	0.999
	80	2.19×10^{-3}	250.0	0.999
	90	2.12×10^{-3}	263.2	0.999
	100	1.93×10^{-3}	270.3	0.999

[a] Adsorption conditions: adsorbent dosage = 0.5 g 2.0 dm^{-3}, agitation rate = 400 rpm, pH = 7.0, particle size = ＜0.074 mm, and temperature = 25 ℃.

Table 4
Pseudo-second order parameters for the adsorption of bisphenol-A onto the activated carbons at various initial pH [a]

Activated carbon	Initial pH	Pseudo-second order		
		k (g mg^{-1}min^{-1})	q_e (mg g^{-1})	R^2
BPL	3	10.28×10^{-3}	237.6	1.000
	5	10.32×10^{-3}	238.6	1.000
	7	10.25×10^{-3}	238.0	1.000
	9	9.05×10^{-3}	239.1	1.000
	11	3.51×10^{-3}	196.1	0.999
PCB	3	3.04×10^{-3}	238.1	0.999
	5	3.30×10^{-3}	232.6	0.999
	7	3.28×10^{-3}	227.3	0.999
	9	3.03×10^{-3}	227.3	0.999
	11	4.38×10^{-3}	140.8	0.999

[a] Adsorption conditions: dosage = 0.5 g 2.0 dm^{-3}, initial concentration = 60 mg dm^{-3}, agitation rate = 400 rpm, particle size = ＜0.074 mm, and temperature = 25 ℃.

Table 5
Pseudo-second order parameters for the adsorption of bisphenol-A onto the activated carbons at various adsorbent dosages [a]

Activated carbon	Adsorbent dosage ($g\ dm^{-3}$)	Pseudo-second order		
		k ($g\ mg^{-1}min^{-1}$)	q_e ($mg\ g^{-1}$)	R^2
BPL	0.05	1.78×10^{-3}	400.0	0.999
	0.10	1.93×10^{-3}	384.6	0.999
	0.15	2.63×10^{-3}	344.8	0.999
	0.20	4.71×10^{-3}	285.7	1.000
	0.25	10.25×10^{-3}	238.0	1.000
PCB	0.05	1.65×10^{-3}	270.3	0.999
	0.10	1.60×10^{-3}	277.8	0.999
	0.15	1.85×10^{-3}	263.2	0.999
	0.20	2.03×10^{-3}	250.0	0.999
	0.25	3.28×10^{-3}	227.3	0.999

[a] Adsorption conditions: initial concentration = 60 $mg\ dm^{-3}$, pH = 7.0, agitation rate = 400 rpm, particle size = ＜0.074 mm, and temperature = 25 ℃.

Table 6
Pseudo-second order parameters for the adsorption of bisphenol-A onto the activated carbons at various adsorbent sizes [a]

Activated carbon	Adsorbent size (mm)	Pseudo-second order		
		k (g mg^{-1}min^{-1})	q_e (mg g^{-1})	R^2
BPL	＜0.074	10.25×10^{-3}	238.0	1.000
	0.074 - 0.125	0.63×10^{-3}	188.7	0.995
	0.125 - 0.250	0.71×10^{-3}	137.0	0.994
PCB	＜0.074	3.28×10^{-3}	227.3	0.999
	0.074 - 0.125	0.88×10^{-3}	137.0	0.996
	0.125 - 0.250	1.66×10^{-3}	80.0	0.996

[a] Adsorption conditions: initial concentration = 60 mg dm^{-3}, pH = 7.0, dosage = 0.5 g 2.0 dm^{-3}, agitation rate = 400 rpm, particle size = ＜0.074 mm, and temperature = 25 ℃.

Table 7
Parameters in the Langmuir and Freundlich adsorption isotherm models of bisphenol-A onto the activated carbons at 25 ℃ [a]

Activated carbon	Langmuir			Freundlich		
	q_m (mg g^{-1})	K_L (dm^3 mg^{-1})	R^2	K_F [mg g^{-1} (dm^3 mg^{-1})$^{1/n}$]	1/n (-)	R^2
BPL	328.3	4.97	0.770	253.8	0.140	0.951
PCB	263.2	1.81	0.854	206.1	0.072	0.963

[a] Adsorption conditions: initial concentration = 60 ~ 100 mg dm^{-3}, adsorbent dosage = 0.5 g 2 dm^{-3}, agitation speed = 400 rpm, particle size = ＜0.074 mm, and pH = 7.0.

.

Figure captions

Fig. 1. Molecular structure of bisphenol-A used as adsorbate in the study.

Fig. 2. Plots of adsorbed bisphenol-A amount versus time onto the activated carbon (BPL) at various agitation speeds (adsorption conditions: adsorbent dosage = 0.5 g 2.0 dm^{-3}, initial concentration = 20 mg dm^{-3}, pH= 7.0, particle size = ＜0.074 mm, and temperature = 25 ℃; Symbols: experimental data, full lines: calculated from pseudo-second order kinetics model).

Fig. 3. Adsorption isotherms of bisphenol-A in aqueous solution onto the activated carbons (i.e., BPL and PCB) at 25 ℃ (Adsorption conditions: dosage = 0.5 g 2.0 dm^{-3}, agitation rate = 400 rpm, particle size = ＜0.074 mm, and pH = 7.0; symbols ●/■: experimental data, full lines: calculated from the Freundlich model, dotted lines: calculated from the Langmuir model).

Fig. 1

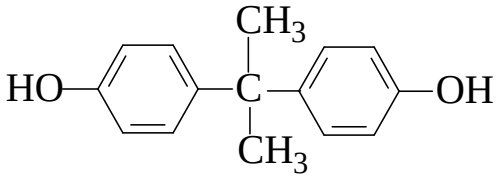

Fig. 2

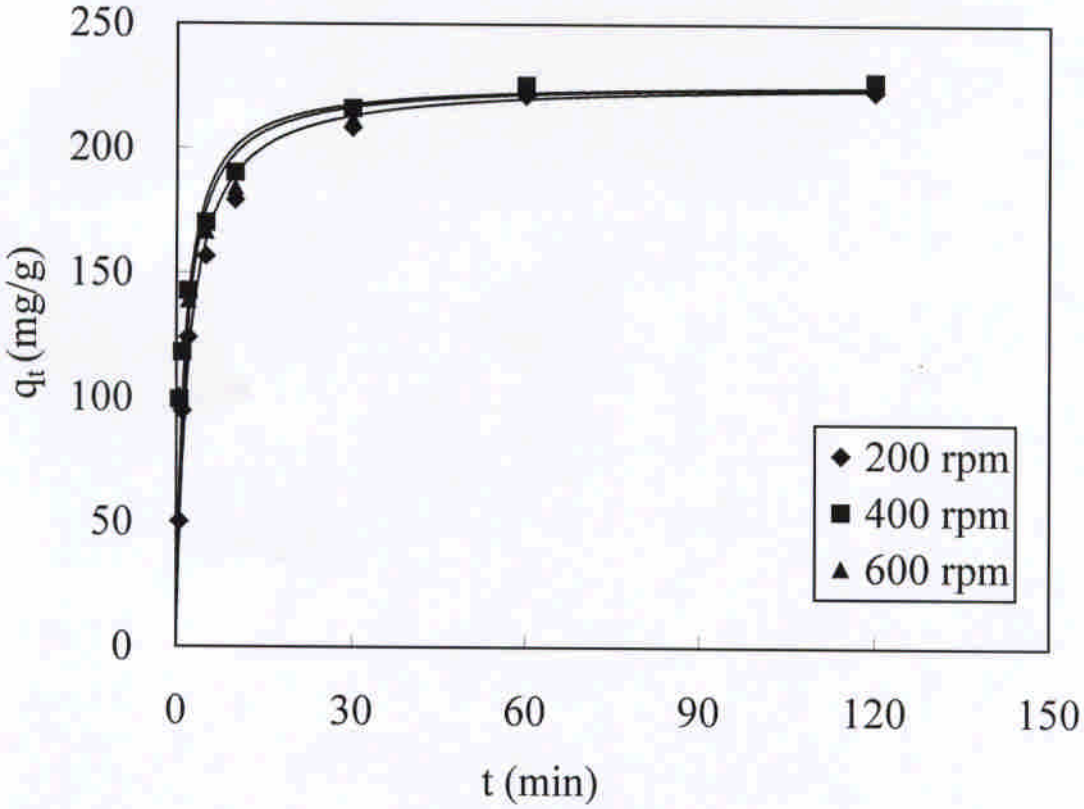
250
200
150
100
50
0
q_t (mg/g)
0
30
60
90
120
150
t (min)
200 rpm
400 rpm
600 rpm

Fig. 3

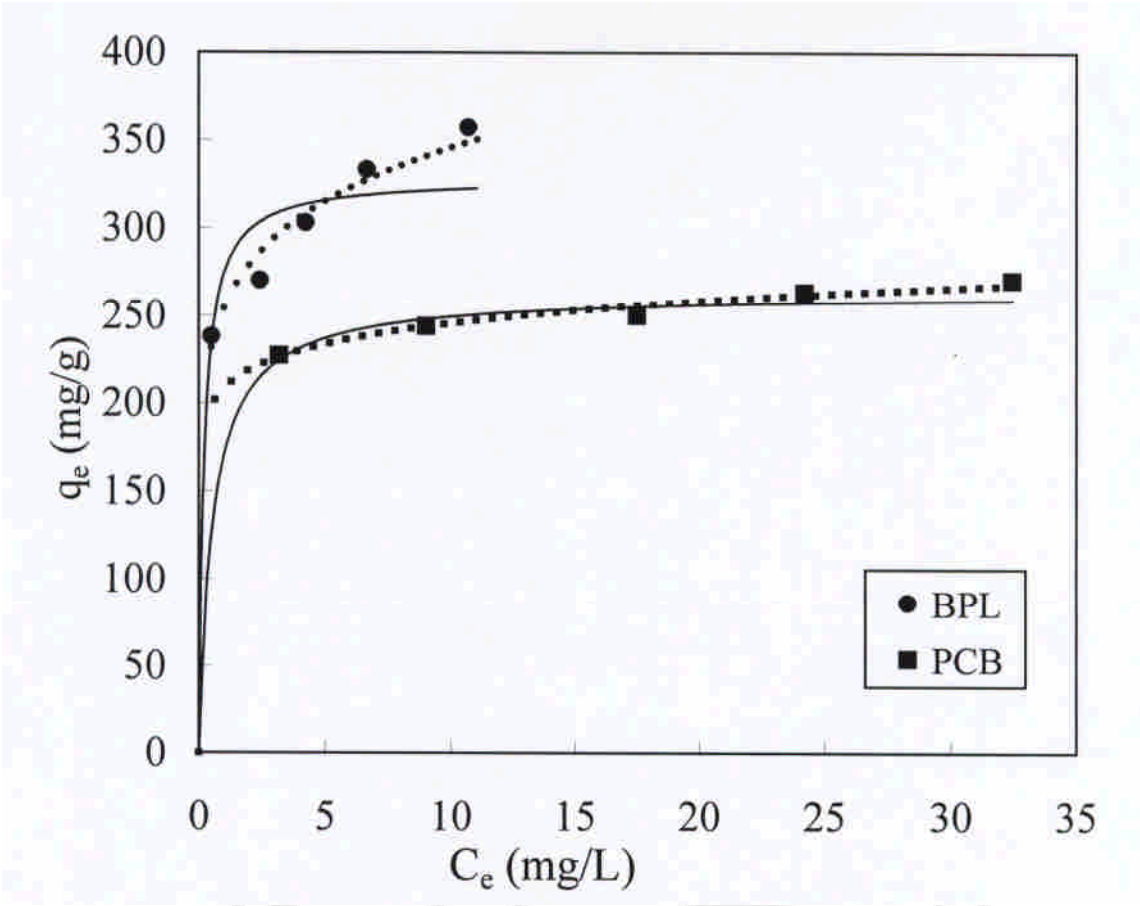
400
350
300
250
200
150
100
50
0
q_e (mg/g)
0
5
10
15
20
25
30
35
C_e (mg/L)
BPL
PCB

可供推廣之研發成果資料表

□ 可申請專利　　■ 可技術移轉　　日期：94 年 10 月 27 日

國科會補助計畫	計畫名稱：廢矽藻土資源再生為多孔性材料及其應用於環境荷爾蒙之處理**(II)** 計畫主持人：　蔡文田 計畫編號：NSC 93-2211-E-041-008　　學門領域：環境工程
技術/創作名稱	多孔性材料製造
發明人/創作人	蔡文田、賴智濰
技術說明	中文： 將廢矽藻土進行氫氟酸化學再生，可使其比表面積由 0.3 m^2/g 提升至 10 m^2/g 以上，可作為吸附材或隔熱材。
	英文： Using chemical regeneration with hydrofluoric acid, the chemically regenerated clays have larger surface areas (≈10 vs. 0.3 m^2/g) than those of the spent diatomaceous earth. The resulting porous mineral can be used as an effective adsorbent or insulation material.
可利用之產業及可開發之產品	製酒工業及油脂工業；吸附劑、隔熱材、觸媒載體等。
技術特點	利用廢矽藻土加以化學再生，可製造出高附加價值材料。
推廣及運用的價值	可作為廢水處理劑、公共建材、助濾劑等。

※　1.每項研發成果請填寫一式二份，一份隨成果報告送繳本會，一份送　貴單位研發成果推廣單位（如技術移轉中心）。

※　**2.本項研發成果若尚未申請專利，請勿揭露可申請專利之主要內容。**